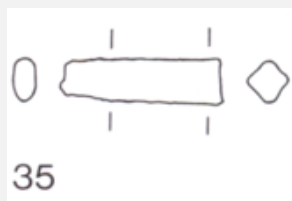


# TANG FRAGMENT OF A KNIFE HR-6246 - TIN BRONZE - LATE BRONZE AGE - SWITZERLAND

<b>Artefact name</b>	Tang fragment of a knife HR-6246
<b>Authors</b>	Marianne. Senn (EMPA, Dübendorf, Zurich, Switzerland) & Christian. Degriigny (HE-Arc CR, Neuchâtel, Neuchâtel, Switzerland)
<b>Url</b>	/artefacts/322/

## ∨ The object



Credit HE-Arc CR.

Fig. 1: Tin bronze tang fragment (after Rychner-Faraggi 1983, plate 35.35),

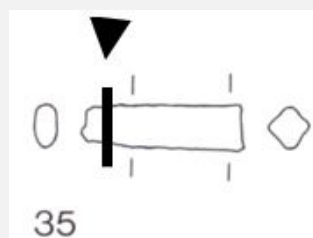
## ∨ Description and visual observation

<b>Description of the artefact</b>	Tang fragment with lake (shiny brown) and terrestrial (granulated green-blue) crust (Fig. 1). Dimensions: L = 2.7cm; Ø = around 5mm; WT = 5.8g.
<b>Type of artefact</b>	Knife
<b>Origin</b>	Hauterive - Champréveyres, Neuchâtel, Neuchâtel, Switzerland
<b>Recovering date</b>	Excavation 1983-1985, object from layer 1 (layer with material from Bronze Age till 20th cent.)
<b>Chronology category</b>	Late Bronze Age
<b>chronology tpq</b>	<input type="text" value="1050"/> B.C. ∨
<b>chronology taq</b>	<input type="text" value="800"/> B.C. ∨
<b>Chronology comment</b>	Hallstatt A/B (1050BC_ 800BC)
<b>Burial conditions / environment</b>	Lake
<b>Artefact location</b>	Laténium, Neuchâtel, Neuchâtel
<b>Owner</b>	Laténium, Neuchâtel, Neuchâtel
<b>Inv. number</b>	Hr 6246
<b>Recorded conservation data</b>	Not conserved

## Complementary information

Nothing to report.

Study area(s)



Credit HE-Arc CR.

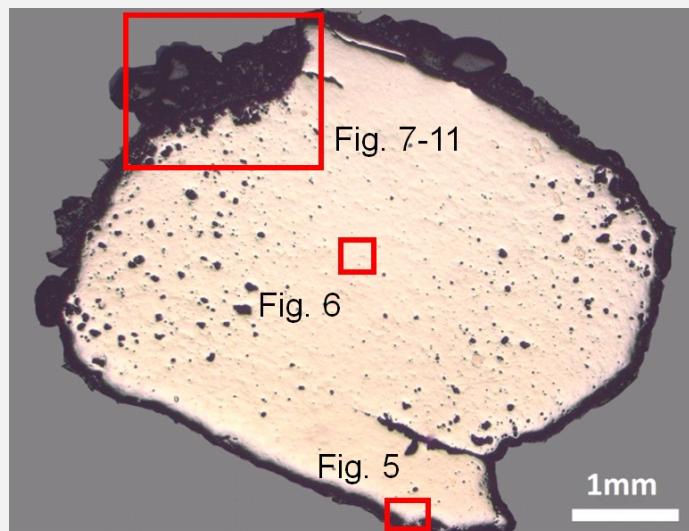
Fig. 2: Location of sampling area,

Binocular observation and representation of the corrosion structure

Stratigraphic representation: none.

MiCorr stratigraphy(ies) – Bi

Sample(s)



Credit HE-Arc CR.

Fig. 3: Micrograph of the cross-section showing the location of Figs. 5 to 11,

Description of sample

The cross-section corresponds to a lateral cut (Fig. 2). The surface is covered with a thick corrosion crust (Fig. 3).

Alloy

Tin Bronze

Technology

Cold worked after annealing

Lab number of sample

MAH 87-197

Sample location

Musées d'art et d'histoire, Genève, Geneva

**Responsible institution** Musées d'art et d'histoire, Genève, Geneva

**Date and aim of sampling** 1987, metallography and corrosion characterisation

#### Complementary information

Nothing to report.

#### Analyses and results

##### *Analyses performed:*

Metallography (etched with ferric chloride reagent), Vickers hardness testing, ICP-OES, SEM/EDS, XRD.

#### Non invasive analysis

#### Metal

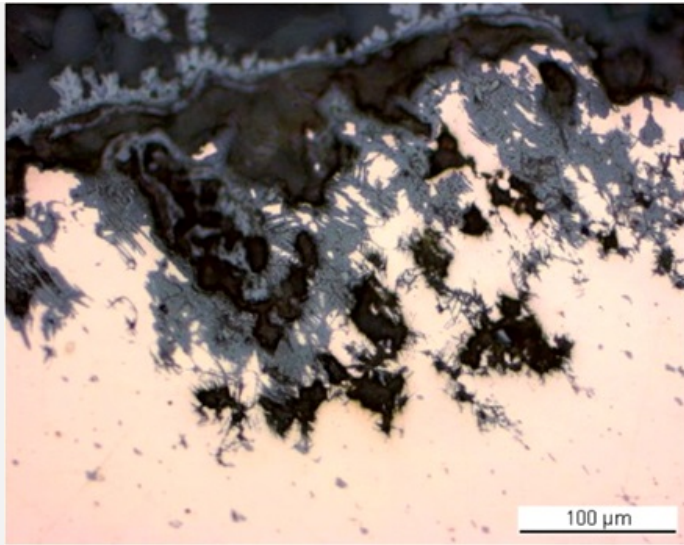
The remaining metal is a tin bronze (Table 1) with high porosity and large cracks both on the left and right edges of the sample (Fig. 3). The metal contains small, elongated copper sulphide (Table 2) and Pb inclusions that are oriented parallel to the cracks. Near the metal surface, slip lines are outlined by the development of intergranular corrosion (Fig. 5). The etched metal shows small, elongated grains with slip lines (Fig. 6). Annealing is visible in areas near the surface. The average hardness of the metal is HV1 145, but significant variations are observed, depending on where the measurements are taken.

Elements	Cu	Sn	Sb	Ni	Pb	As	Ag	Co	Fe	Zn
mass%	89.85	8.02	0.60	0.55	0.34	0.34	0.18	0.10	0.02	0.01

Table 1: Chemical composition of the metal. Method of analysis: ICP-OES, Laboratory of Analytical Chemistry, Empa.

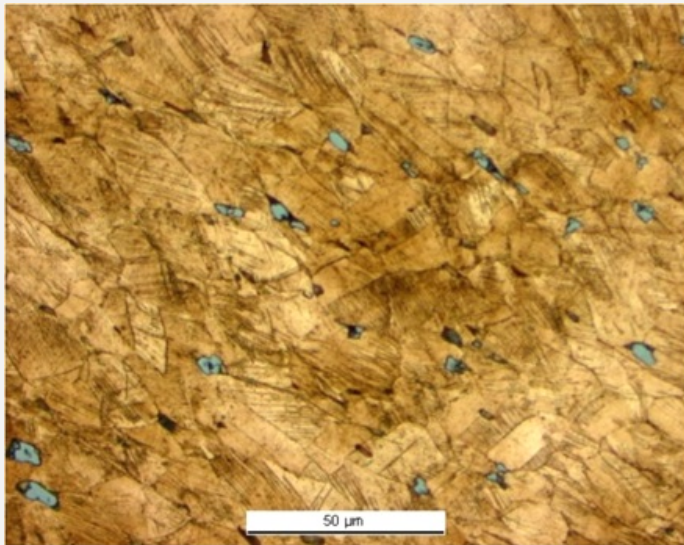
Elements	O	S	Cu	Total
mass%	0.9	20	77	98

Table 2: Chemical composition of inclusions. Method of analysis: SEM/EDS, Laboratory of Analytical Chemistry, Empa.



Credit HE-Arc CR.

Fig. 5: Micrograph of the metal sample from Fig. 3 (inverted and reversed picture, detail), unetched, bright field. Corrosion products are in dark-grey whereas the metal is in pink. Slip lines are outlined by the development of intergranular corrosion,



Credit HE-Arc CR.

Fig. 6: Micrograph of the metal sample from Fig. 3 (detail), etched, bright field. We observe elongated grains with slip lines as well as grey copper sulphide inclusions,

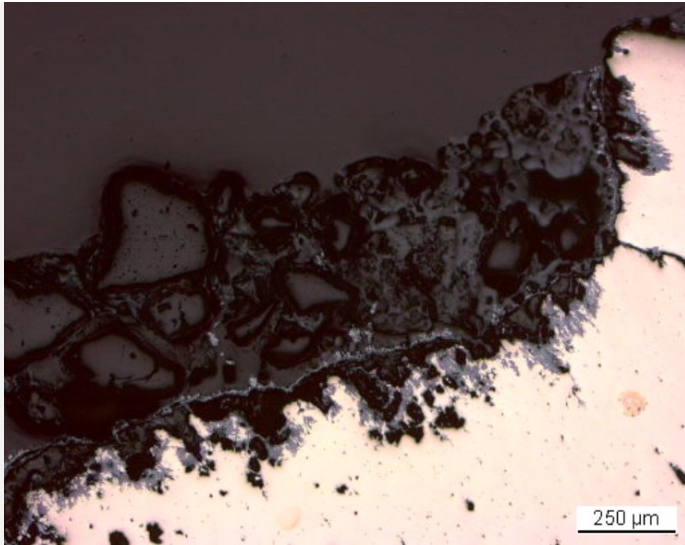
<b>Microstructure</b>	Elongated grains + strain lines with pores
<b>First metal element</b>	Cu
<b>Other metal elements</b>	Sn

#### Complementary information

Nothing to report.

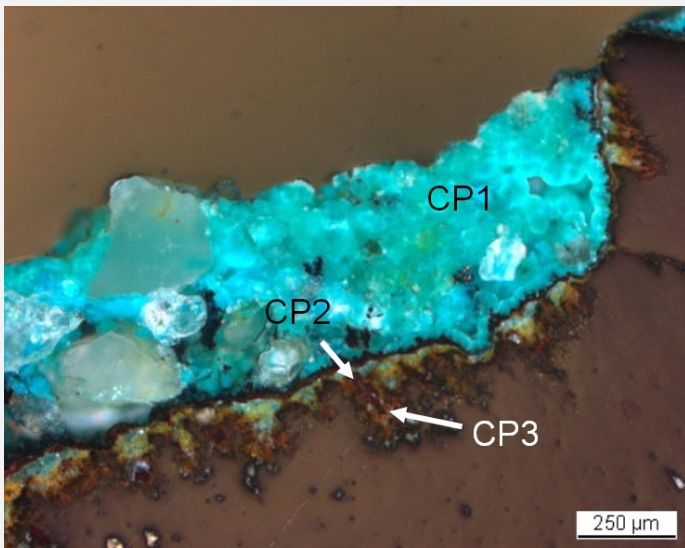
#### ✖ Corrosion layers

The corrosion crust has a thickness between 0.1mm and 0.7mm (Fig. 3). In bright field (Fig. 7), one can observe that the metal has been replaced by light-grey corrosion products. Adjacent to the metal is a thick, heterogeneous, dark-grey layer with a band of light-grey corrosion products. In polarised light (Fig. 8), all corrosion products which were previously light-grey appear brown-orange, the dark-grey layer turquoise. The elemental chemical distribution of the SEM images (Figs. 9 and 10) reveals that the inner corrosion products are Sn-rich whereas the adjacent band is Cu and S-rich (Fig. 11). The outer layer contains large inclusions (quartz and others, Si, Al and Na, see Figs. 10-11) and is most probably composed of malachite/ $\text{Cu}_2(\text{CO}_3)(\text{OH})_2$  (only Cu and O are detected – Fig. 11). S is distributed throughout this layer. XRD analyses indicated the presence of posnjakite/ $\text{Cu}_4\text{SO}_4(\text{OH})_6\text{H}_2\text{O}$ , chalcocite/ $\text{Cu}_2\text{S}$  and djurleite/ $\text{Cu}_{1.93}\text{S}$  (Schweizer 1994).



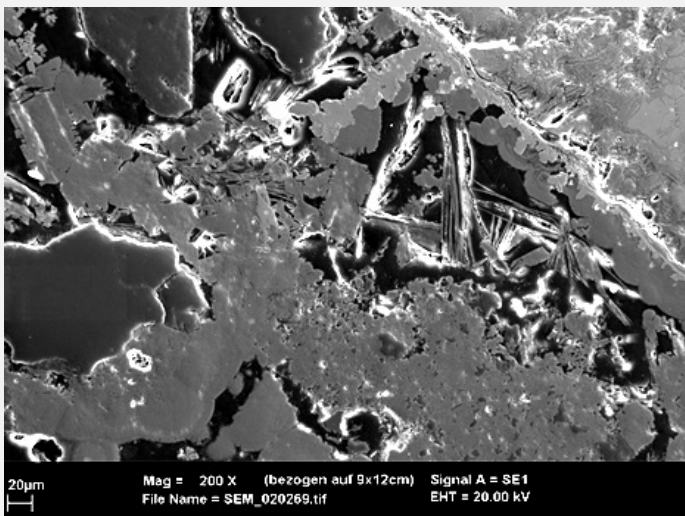
Credit HE-Arc CR.

Fig. 7: Micrograph of the metal sample from Fig. 3 (detail), unetched, bright field. The inner light-grey corrosion products extend into the metal surface (in pink) and appear as a line within the dark-grey corrosion layer,



Credit HE-Arc CR.

Fig. 8: Micrograph similar to Fig. 7 and corresponding to the stratigraphy of Fig. 4, polarized light. One can see that large mineral features are incorporated only in the corrosion layers above the brown-orange corrosion band,



Credit HE-Arc CR.

Fig. 9: SEM image (detail of Fig. 7), SE-mode. From bottom to top right: the thick, porous outer corrosion layer, the light-grey band and the remaining metal,

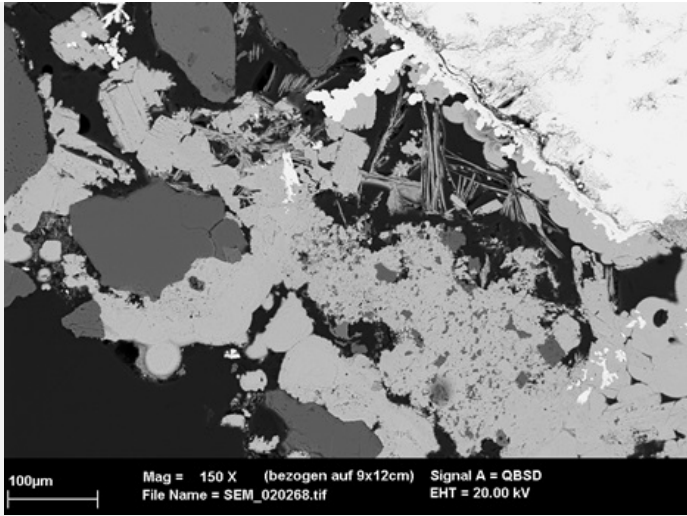


Fig. 10: SEM image, similar to Fig. 9, BSE-mode,

Credit HE-Arc CR.

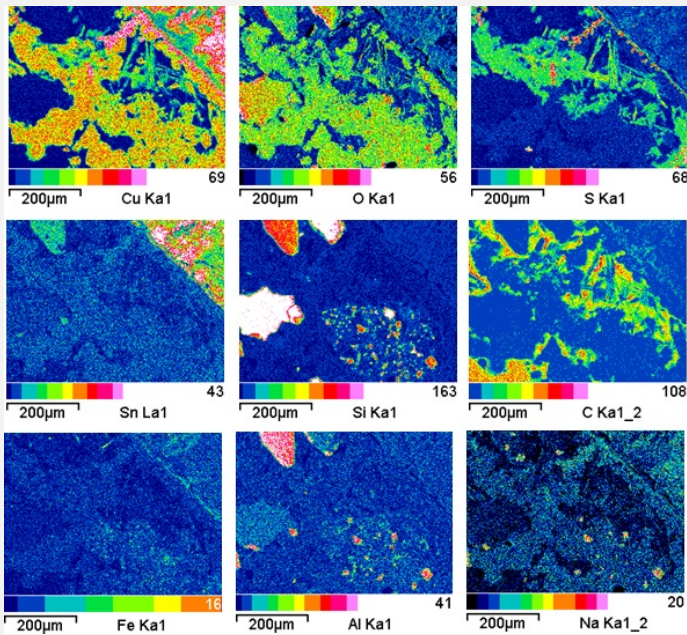


Fig. 11: EDS elemental chemical distribution of the SEM image of Fig. 9. Method of examination: SEM/EDS, Laboratory of Analytical Chemistry, Empa,

Credit Empa.

**Corrosion form** Uniform - transgranular

**Corrosion type** Type I (Robbiola)

**Complementary information**

Nothing to report.

∨ MiCorr stratigraphy(ies) – CS

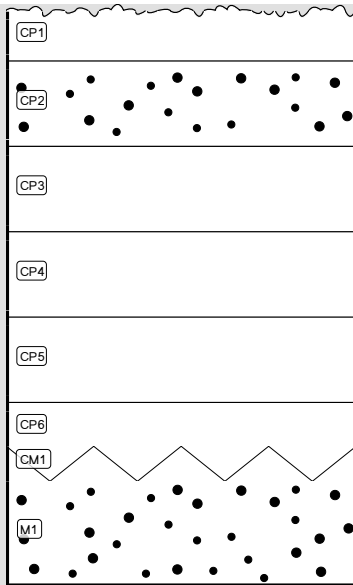


Fig. 4: Stratigraphic representation of the object in cross-section using the MiCorr application. This representation can be compared to Fig. 8.

#### ✧ Synthesis of the binocular / cross-section examination of the corrosion structure

Corrected stratigraphic representation: none.

#### ✧ Conclusion

The tang fragment is made from a leaded bronze and has been cold worked on the top surface after annealing. The SEM/EDX examination and past XRD analyses indicate the presence of chalcopyrite in the corrosion crust, typical of lake context (Schweizer 1994), enriched with Sn close to the metal surface and depleted of Cu on the outer surface. This object was certainly abandoned rather quickly in an anaerobic, humid and S and Fe-rich environment, favouring then the formation of chalcopyrite. The limit of the original surface most probably lies between the Sn-rich inner layer and the Fe and S-rich outer layers. The presence of iron oxides on top of the copper corrosion crust has not yet been explained. The corrosion is a type 1 according Robbiola et al. 1998.

#### ✧ References

##### *References on object and sample*

##### **References object**

1. Rychner-Faraggi A-M. (1993) Hauterive – Champréveyres 9. Métal et parure au Bronze final. Archéologie neuchâteloise, 17 (Neuchâtel).

##### **References sample**

2. Rapport d'examen, Laboratoire Musées d'art et d'histoire, Geneva GE (1987), 87-194 à 197

3. Schweizer, F. (1994) Objets en bronze provenant de sites lacustre: de leur patine à leur biographie. In: L'œuvre d'art sous le regard des sciences (éd. Rinuy, A. and Schweizer, F.), 143-157.

##### *References on analytic methods and interpretation*

4. Robbiola, L., Blengino, J-M., Fiaud, C. (1998) Morphology and mechanisms of formation of natural patinas on archaeological Cu-Sn alloys, Corrosion Science, 40, 12, 2083-2111.